Performance of Thermoelectric Generator in the Combustion of Wood Charcoal with Various Fan Powers

Andi Ibrahim Soumi[1], Bagus Radiant Utomo[1], Patna Partono[1], Tri Tjahjono[1], Nugroho Tri Atmoko[2], and Amin Sulistyanto[1](✉)

[1] Department of Mechanical Engineering, Faculty of Engineering, Universitas Muhammadiyah Surakarta, Jl. A. Yani Tromol Pos 1 Pabelan Kartasura, Surakarta 57102, Indonesia
{pp136,tt142,as141}@ums.ac.id

[2] Faculty of Engineering, Sekolah Tinggi Akademi Warga Surakarta, Jl. Raya Solo-Baki Km.2 Kwarasan, Solo Baru, Surakarta, Sukoharjo, Indonesia
nugroho.ta@sttw.ac.id

Abstract. Thermoelectric material can convert waste heat from the combustion gas into electrical energy. The objective of this work was to study the effect of fan power on the electrical output of a thermoelectric generator used in the combustion of wood charcoal. The side wall of the combustion stove has thermoelectric modules mounted on it. The cold side of the thermoelectric module is fitted with a water block with water flowing water. The temperature and power sensors are controlled using a microcontroller. The fan power was varied using 0.4, 0.6, and 0.8 W to blow the outdoor air into the chamber. The results showed that an increased power fan increases the temperature difference of the TEG hot-cold sides, which results in the TEG's power increase. The efficiency, however, decreases with an increase in fan power. The present work is expected to improve the design of the chamber for harvesting the energy released by charcoal combustion.

Keywords: Thermoelectric generator · wood charcoal · fan powers · TEG power · Efficiency

1 Introduction

Environmental pollution originating from pollutant exhaust gases from burning fossil energy, such as in power plants, and the increase in costs for the use of electrical energy are significant problems faced in today's modern era [1]. As a result of the increase in pollutants that cause global warming, people need to reduce pollutants using renewable energy [2]. One of the considerations for replacing fossil energy is using new or renewable energy [3]. Efforts to reduce energy consumption and pollutants have been carried out in various studies, such as using waste heat energy, comfort building, and alternative heat sources [4–8]. The recovery of the wasted heat energy can encourage energy and fuel savings [9]. Thermoelectric generators (TEG) can use waste heat for electrical power [10, 11]. The thermoelectric generator system offers the advantage of

T. P. Syawitri et al. (Eds.): MEST 2022, AER 222, pp. 210–219, 2023.
https://doi.org/10.2991/978-94-6463-134-0_20

the temperature difference on both TEG sides so that it can generate electrical energy directly without moving parts [12]. TEG operates without noise, has a light mass, and takes minimum maintenance [13]. The Seebeck effect takes a conversion of temperature differences into electrical energy [14].

Thermoelectric modules on stoves can produce electrical energy by utilizing heat so that temperature differences occur [15, 16]. Champier et al. [17] conducted research by applying a thermoelectric generator to a biomass stove as a power generator to turn on a fan and lighting. Using TEG on a biomass stove can generate 6 W of electrical power. Mal et al. [18] designed and tested thermoelectric modules applied to biomass stoves. The generated electrical energy turns on DC fans, and the excess power is stored in the battery. The results of measuring the temperature difference are directly proportional to the electrical power generated by the TEG. Lertsatitthanakorn [19] researched thermoelectric modules that are applied to combustion furnaces by installing thermoelectric modules on the side walls of the combustion furnace. The wall side of the stove is used as the hot side of the TEG module, and a fin-type heat sink is used as the cold side of the TEG module. Research on the TEG module in this combustion furnace reveals that the output power and efficiency depend on the temperature difference between the hot side and the cold side of the TEG module. Although several reports have been found regarding the use of TEG in stoves, studies on the effect of air velocity on burning charcoal as a fuel on the output of TEG still need to be made available. This study aimed to determine the impact of fan power with 0.4, 0.6, and 0.8 W on the TEG output in wood charcoal burning. The result of this study is expected to improve the design of the combustion chamber used in a household.

2 Theoretical Considerations

If a TEG is heated on one side and simultaneously cooled on the other, then the electrons on the hot side have more kinetic energy than those on the cold side. Electrons moving on the hot side become positively charged, while electrons on the cold side are negatively charged [20]. In such a condition, the conductance boundary lies between a hot and cold temperature source. The n-type material can deliver electrons to the conduction area called a donor. In contrast, the p-type functions as an electron acceptor [21]. Figure 1 explains the working principle of a thermoelectric generator by describing the transfer of electrons from the hot side to the cold side. The thermoelectric generator module works with the Seebeck effect, where the temperature difference between the hot and cold sides of the TEG module is converted into electrical energy [22]. Electric current through two materials can absorb heat or release heat per unit of time as the stability of the chemical structure of the two materials is known as the Peltier Effect. The Peltier effect occurs because the energy on electrons participates in the transfer of electric currents from different materials as conductors [20].

Thomson explained that there is an indication that the current is flowing through and unbalanced with the conductor being heated so that energy is consumed or builds up in the metal structure. The Thomson effect shows heat loss by current passing through a substance and heat transfer. The amount of heat absorbed or released in one ampere of current in one second at different temperatures is called the Thomson Coefficient

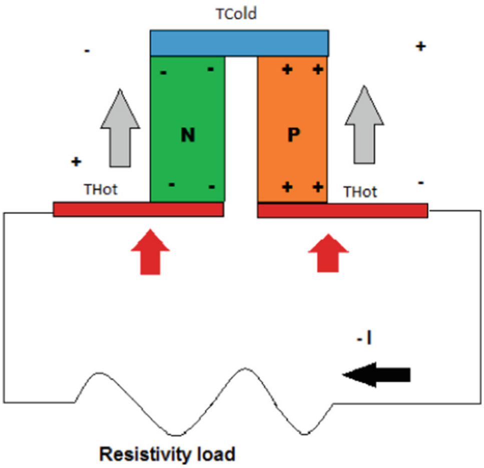

Fig. 1. Schematic diagram of thermoelectric generator

[20]. German physicist Thomas Johann Seebeck discovered a potential difference called the Seebeck voltage that occurs at the ends of a conductor where the two ends of the conductor have a temperature difference. The Seebeck voltage is directly proportional to the temperature difference value, written in Eq. (1).

$$E = \alpha \cdot \Delta \mathrm{T} \tag{1}$$

where α is the Seebeck coefficient with a unit of V/K [23].

The Seebeck coefficient needs to be as high as possible to generate power with a high conversion rate. The electrical and thermal conductivity of semiconductor materials expressed as the value of the figure of merit (Eq. 2) substantially impacts a TEG's performance [24].

$$Z = \frac{\sigma \alpha^2}{\lambda} \tag{2}$$

where σ and λ stand for the semiconductor materials' relative electrical and thermal conductivity, respectively. Some works presume that the figure of merit, derived without considering temperature change, is unchanged.

Equations (3) and (4) can be used to indicate the rate of heat absorption and heat loss in a TEG's hot and cold sides, respectively, when the TEG is exposed to a heat source on its hot side.

$$\mathrm{Q_H} = \mathrm{K}(\mathrm{T_H} - \mathrm{T_C}) + (\alpha_p - \alpha_n)\mathrm{I}\mathrm{T_H} - \frac{RI^2}{2} \tag{3}$$

$$\mathrm{Q_C} = \mathrm{K}(\mathrm{T_H} - \mathrm{T_C}) + (\alpha_p - \alpha_n)\mathrm{I}\mathrm{T_C} - \frac{RI^2}{2} \tag{4}$$

where I is the current flowing through the thermoelement materials, and α_p and α_n are the p- and n-type semiconductor materials' respective Seebeck coefficients.

(a) (b) (c)

Fig. 2. Experimental components (a). Charcoal, (b). TEG module, and (c) Fan

The thermoelement's output power is expressed in Eq. (5).

$$W = V \times I = Q_H - Q_C \tag{5}$$

When a current flows through the TEG circuit, the power output is expressed in Eq. (6).

$$W = (\alpha \Delta T)^2 \frac{R_L}{(R + R_L)^2} \tag{6}$$

where R_i and R_L are the internal resistance and the load resistance, respectively.

The efficiency is calculated using Eq. (7).

$$\mu TE_{max} = \frac{\Delta T}{T_H} \cdot \frac{\sqrt{1 + ZT} - 1}{\sqrt{1 + ZT} + \frac{T_C}{T_H}} \tag{7}$$

3 Methods

Figure 2 shows the wood charcoal, TEG module, and fan. The thermoelectric generator was applied to indirectly absorb the heat from the combustion of wood charcoal. The hot side of the TEG module receives the heat from the wall of the combustion chamber. TEG uses a cooling water system with a water block on the cold side. The TEG module used in this study uses the type SP 1848 27145 SA. Table 1 shows the specifications of the TEG type SP 1848 27145 SA. The fan uses powers of 0.4, 0.6, and 0.8 W.

Figure 3 describes the design of the combustor used in this study. The TEG arrangement is attached to the combustor wall. Air enters through the bottom channel to the combustion chamber, as shown in Fig. 4. The hot side of the thermoelectric module uses an aluminum plate mounted as the heat conductor. A water block is attached for the cooling system on the cold side of the thermoelectric module. In the TEG arrangement, thermocouples are applied to measure the hot side temperature and cold side temperatures of the TEG module. The data logger used to collect the data on temperature, voltage, and electric current in this study uses the Arduino Mega 2560. The sensor that reads the temperature uses the MAX 6675 sensor. The working sensors send signals to the data logger. The measured data is displayed on the serial monitor.

Table 1. The manufacturer's specification of the thermoelectric generator

Parameters	Unit	Remark
Dimension of TEG		
a. length	mm	40
b. width	mm	40
c. thickness	mm	3.9
d. mass	g	3.6
Type of material		
a. Hot Side and Cold Side	–	Al2O3
b. Conductor	–	Cu
c. Semiconductor p-leg	–	Bi2 Te3
d. Semiconductor n-leg	–	Bi_2 Te_3
e. Joining	–	Bi Sn
Dimension:		
a. Hot Side and Cold Side l × w × t	mm	40 × 40 × 0.75
b. Material Konduktor l × w × t	mm	4 × 1.58 × 0.45
c. Semikonduktor p-leg l × w × t	mm	1 × 1 × 1.4
d. Semikonduktor n-leg l × w × t	mm	1 × 1 × .4
e. Joining	–	0.05
Physical Parameters:		
a. Number Semiconductor p-type	–	110
b. Number Semiconductor n-type	–	110
c. Operation Temperature	°C	0–150
d. Maximum Temperature Operation	°C	300
e. Seebeck Coefficient	V/K	0.054
f. Internal Resistivity at ΔT 110 °C	Ohm	33

4 Results and Discussion

Figure 5 shows the temperature profile of TEG's hot-cold sides using a variation of fan power. The three graphs show the temperature profile of the hot side and cold side of the TEG against time using a power of 0.4, 0.6, and 0.8 W. The increase in temperature on the hot side is followed by the temperature on the cold side and vice versa. In the use of 0.4 W fan power, the highest temperature on the hot side is 176.08 ˚C, and the temperature on the cold side is 77.33 ˚C. Using 0.6 W fan power produces the highest hot side temperature at 179.92 ˚C and cold side temperature at 80.42 ˚C. In the 0.8 W fan power, the maximum hot side temperature is 190 ˚C, and the cold side temperature is 91 ˚C. This result shows that the greater the fan power, the higher the temperature on

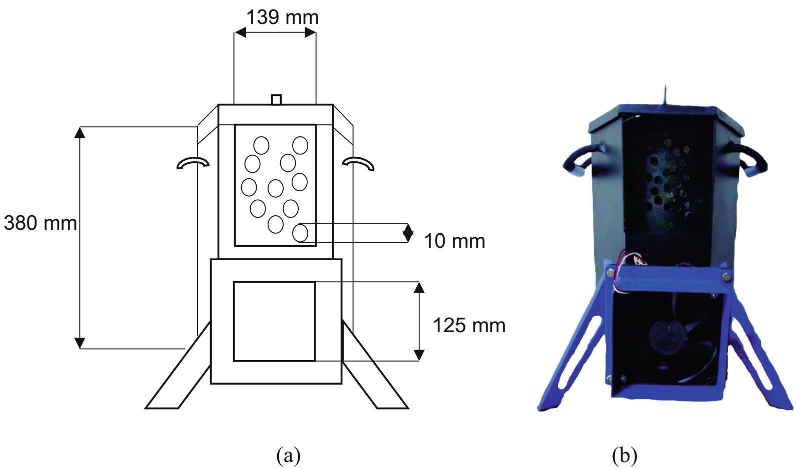

Fig. 3. The combustion chamber (a) schematic diagram, (b) photograph

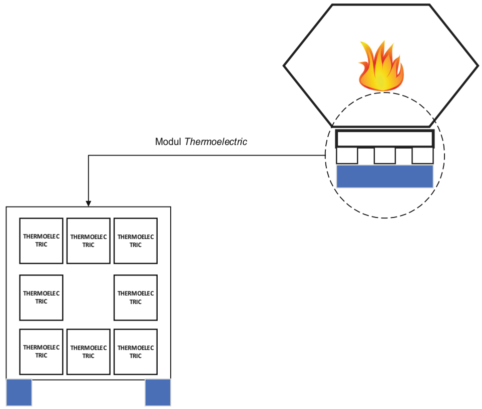

Fig. 4. The schematic diagram of the TEG arrangements

the hot and cold sides. Comparing the various fan powers, an increase in the fan power increases the temperature of the TEG.

Figure 6 shows the power profile concerning temperature changes for each variation of fan powers. Variations in the fan power with 0.4, 0.6, and 0.8 W cause differences in airflow. The higher the energy used in the fan, the higher the fan flow rate. A higher fan flow rate causes a higher heat flow rate so that the hot side temperature becomes higher, which causes the temperature change between the hot side and the cold side to be higher. The increase in fan power usage is also accompanied by increased power generated. Using a 0.4 W fan power produces a maximum power of 2.82 W at a temperature difference of 99.17 °C. the use of 0.6 W fan power is capable of producing a peak power of 4.56 W at a temperature change point of 99.42°C. In comparison, using a 0.8 W fan

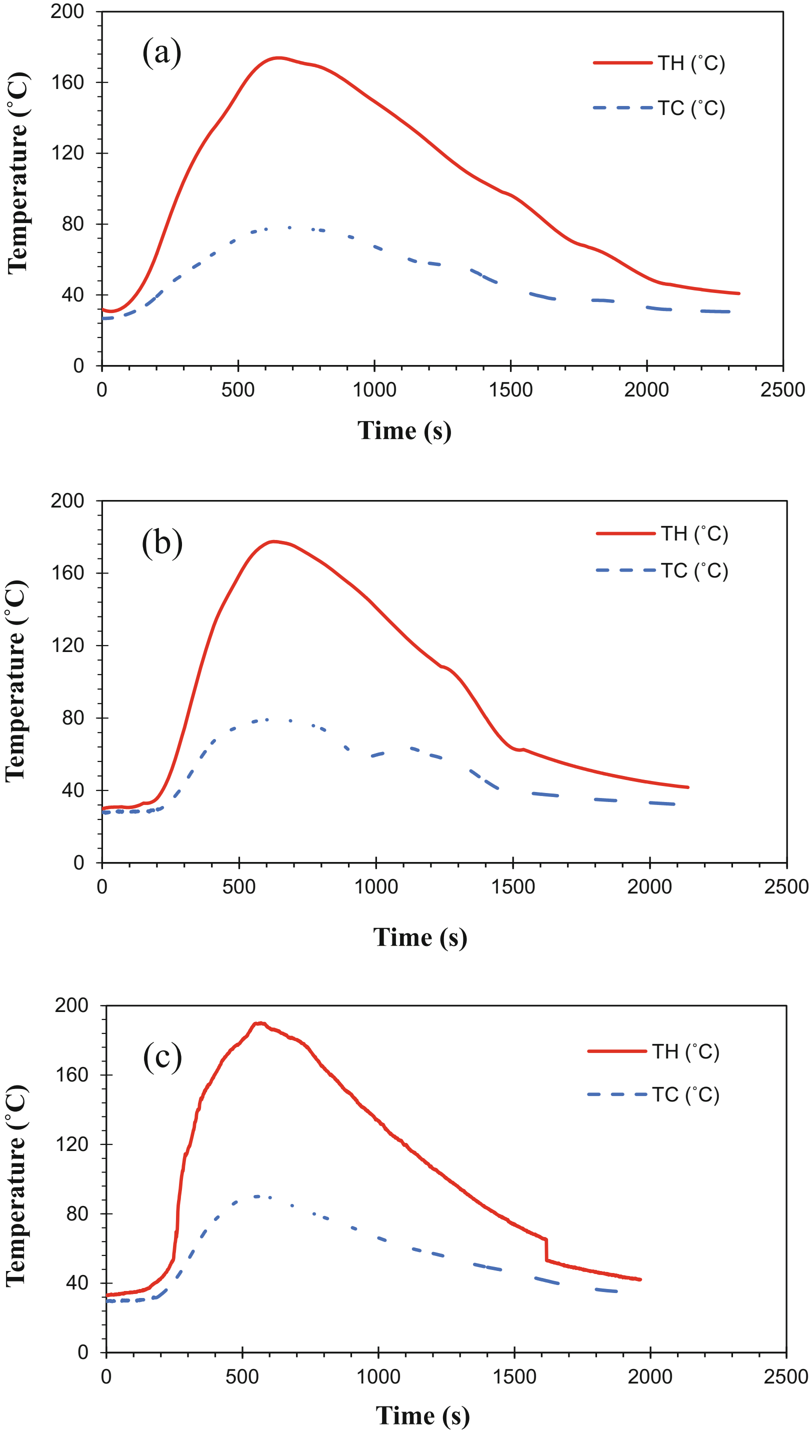

Fig. 5. Temperature profile of TEG's hot-cold sides using a fan power of (a) 0.4 W, (b) 0.6 W, and (c) 0.8 W

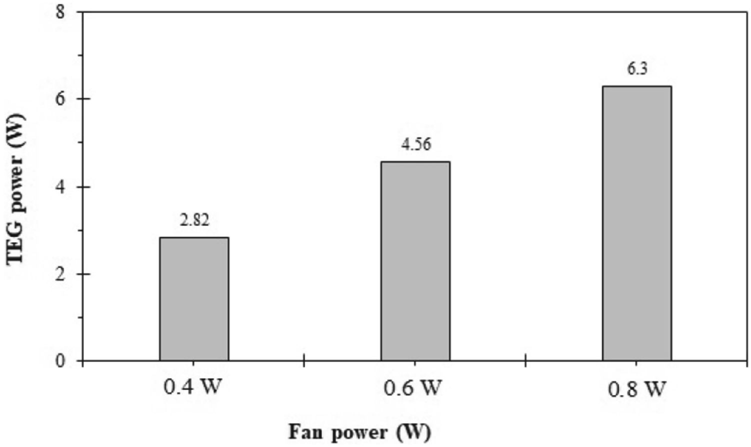

Fig. 6. Maximum power generated by TEG with various fan powers

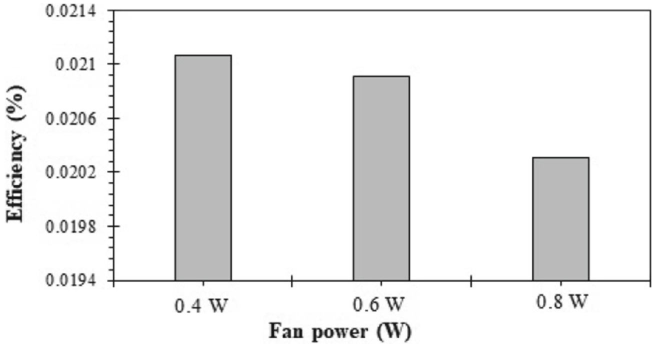

Fig. 7. Maximum efficiency of the TEG system with various fan powers

power variation has a maximum power of 6.3 W at a temperature change point of 102˚C. This result shows that the greater the fan power, the higher the energy obtained.

Figure 7 shows the TEG efficiency for each use of fan power variations of 0.4, 0.6, and 0.8 W. The efficiency of the TEG system for differences in air velocity shows a slight difference. In the fan power of 0.4 W, the efficiency is 0.0210%. In the 0.6 W fan power at the highest temperature difference of 99.42 ˚C, the efficiency value is 0.0209%, while using 0.8 W fan power variations at the highest temperature of 102˚C obtains an efficiency of 0.0203%. This result shows that the greater the fan power variations, the more efficiency experiences a slight decrease.

5 Conclusion

This work has successfully investigated the effect of fan power on the electrical output and efficiency of the thermoelectric module that received heat from the combustion of wood charcoal. The result of the study showed that an increase in fan power produces higher TEG power and efficiency. The investigated fan power using 0.4 W, 0.6 W, and 0.8 W has 99.17 ˚C, 99.42 ˚C, and 102 ˚C, which results in the TEG power of 2.82 W, 4.56 W, and 6.3 W, respectively. The increasing fan power decreases the efficiency of the systems by 0.021%, 0.0209%, and 0.0203%. This work improves the understanding of the energy conversion using thermoelectric material that is expected to enhance the TEG's performance in its application at various high-temperature.

Acknowledgement. The authors would like to thank the funding provided by Research and Innovation Institute, Universitas Muhammadiyah Surakarta, through a master thesis research scheme with grant Number: 274.10/A.3-III/LRI/XI/2022. An invaluable discussion with Dr. Riyadi is much appreciated.

References

1. K. T. Wojciechowski, M. Borcuch, M. Musial, and P. Wyzga, "A testbed for performance studies of gas – liquid thermoelectric generators for waste heat harvesting," Measurement, vol. 203, no. September, p. 111933, 2022.
2. B. Pfeiffelmann and A. C. Benim, "Water-Cooled Thermoelectric Generators for Improved Net Output Power : A Review," 2021.
3. L. Tian, L. Chen, T. Ren, Y. Ge, and H. Feng, "Optimal distribution of heat exchanger area for maximum efficient power of thermoelectric generators," Energy Reports, vol. 8, pp. 10492–10500, 2022.
4. H. H. Al-Kayiem, K. Koh, T. W. B. Riyadi, and M. Effendy, "A comparative review on greenery ecosystems and their impacts on sustainability of building environment," Sustain., vol. 12, no. 20, pp. 1–26, 2020.
5. W. He, G. Zhang, X. Zhang, J. Ji, G. Li, and X. Zhao, "Recent development and application of thermoelectric generator and cooler," Appl. Energy, vol. 143, pp. 1–25, 2015.
6. Sarjito and T. W. B. Riyadi, "A parametric study of wind catcher model in a typical system of evaporative cooling tower using CFD," Appl. Mech. Mater., vol. 660, pp. 659–663, 2014.
7. T. W. B. Riyadi, T. Zhang, and Sarjito, "Microstructure and adhesion of NiAl/Al and NiAl/Ni coatings formed by SHS process," Appl. Mech. Mater., vol. 660, pp. 185–189, 2014.
8. T. W. B. Riyadi, Sarjito, and P. Partono, "The effect of compaction pressures on the microstructure and properties of NiAl/Ti formed by SHS process," ARPN J. Eng. Appl. Sci., vol. 11, no. 10, pp. 6615–6618, 2016.
9. Y. Zhao, M. Lu, L. Yue, L. Xie, and M. Ge, "ScienceDirect Influence of porous plate position on thermoelectric generator," Energy Reports, vol. 8, pp. 1045–1050, 2022.
10. J. Chung, B. Ryu, and H. Seo, "Nonlinear Analysis : Real World Applications Unique temperature distribution and explicit efficiency formula for one-dimensional thermoelectric generators under constant Seebeck coefficients," Nonlinear Anal. Real World Appl., vol. 68, p. 103649, 2022.
11. N. T. Atmoko, I. Veza, and T. W. B. Riyadi, "Study On The Energy Conversion In The Thermoelectric Liquefied Petroleum Gas Cooking Stove With Different Cooling Methods," Int. J. Eng. Trends Technol., vol. 69, no. 1, pp. 185–193, 2021.
12. C. Yu and K. T. Chau, "Thermoelectric automotive waste heat energy recovery using maximum power point tracking," Energy Convers. Manag., vol. 50, no. 6, pp. 1506–1512, 2009.

13. T. Young, A. Negash, and G. Cho, "Direct contact thermoelectric generator (DCTEG): A concept for removing the contact resistance between thermoelectric modules and heat source," Energy Convers. Manag., vol. 142, pp. 20–27, 2017.
14. H. Ruan, H. Xie, J. Wang, J. Liao, and L. Sun, "Case Studies in Thermal Engineering Numerical investigation and comparative analysis of nanofluid cooling enhancement for TEG and TEC systems," Case Stud. Therm. Eng., vol. 27, no. August, p. 101331, 2021.
15. Y. S. H. Najjar and M. M. Kseibi, "Thermoelectric stoves for poor deprived regions – A review," Renew. Sustain. Energy Rev., vol. 80, no. May, pp. 597–602, 2017.
16. T. W, B. Riyadi, B. Radiant, M. Effendy, A. Tri, and H. H. Al-kayiem, "Effect of thermal cycling with various heating rates on the performance of thermoelectric modules," Int. J. Therm. Sci., vol. 178, no. March, p. 107601, 2022.
17. D. Champier, J. P. Bedecarrats, M. Rivaletto, and F. Strub, "Thermoelectric power generation from biomass cook stoves," Energy, vol. 35, no. 2, pp. 935–942, 2010.
18. R. Mal, R. Prasad, V. K. Vijay, and A. S. Technology, "Design and Testing of Thermoelectric Generator embedded Clean Forced Draft Biomass Cookstove," 2015.
19. C. Lertsatitthanakorn, "Electrical performance analysis and economic evaluation of combined biomass cook stove thermoelectric (BITE) generator," vol. 98, pp. 1670–1674, 2007.
20. H. Jouhara et al., "International Journal of Thermo fl uids Thermoelectric generator (TEG) technologies and applications," vol. 9, 2021.
21. P. T. Mcknight, "Finite Element Analysis of Thermoelectric Systems with Applications in Self Assembly and Haptics," 2010.
22. K. Karthick, S. Suresh, G. C. Joy, and R. Dhanuskodi, "Energy for Sustainable Development Experimental investigation of solar reversible power generation in Thermoelectric Generator (TEG) using thermal energy storage," Energy Sustain. Dev., vol. 48, pp. 107–114, 2019.
23. S. Dis, "Microcontroller-based test system for determining the P-N type and Seebeck coefficient of the thermoelectric semiconductors," vol. 139, pp. 361–369, 2019.
24. E. Ramos, J. Silva-Valencia, R. Franco, and M. S. Figueira, "The thermoelectric figure of merit for the single electron transistor," Int. J. Therm. Sci., vol. 86, pp. 387–393, 2014.